Brain Pathology ISSN 1015-6305

RESEARCH ARTICLE

Claudin 6 Is a Positive Marker for Atypical Teratoid/Rhabdoid Tumors

Diane K. Birks[1,4]; Bette K. Kleinschmidt-DeMasters[1,3]; Andrew M. Donson[2,4]; Valerie N. Barton[2,4]; Sean A. McNatt[1,4]; Nicholas K. Foreman[1–4]; Michael H. Handler[1,4]

[1] Departments of Neurosurgery, [2] Pediatrics, and [3] Pathology and Neurology, Anschutz Medical Campus, University of Colorado at Denver, Aurora, Colo.
[4] The Children's Hospital, Aurora, Colo.

Keywords
Affymetrix, atypical teratoid/rhabdoid tumor, BAF47, brain tumor, *claudin 6*, *CLDN6*, hSNF5, *INI1*, microarray, monosomy 22, pediatric, SMARCB1.

Corresponding author:
Diane K. Birks, MS, Department of Neurosurgery, University of Colorado at Denver, Mail stop 8302, PO Box 6511, Aurora, CO 80045 (E-mail: *diane.birks@uchsc.edu*)

Received 11 September 2008; accepted 12 November 2008.

Presented in abstract format at the 13th International Society for Pediatric Neuro-oncology Meeting, Chicago, July 2008.

doi:10.1111/j.1750-3639.2008.00255.x

Abstract

Atypical teratoid/rhabdoid tumors (AT/RTs) are highly aggressive pediatric brain tumors characterized by the presence of rhabdoid cells and negative immunostaining for INI1 (BAF47). Histogenesis is unknown and diagnosis can be challenging because of their extreme morphological and immunophenotypic heterogeneity. Currently no signature markers other than INI1 loss have been identified. To search for possible candidate proteins of interest in AT/RTs, Affymetrix GeneChip® microarrays were utilized to investigate nine AT/RTs vs. 124 other tumor samples. The most distinctive gene identified was *claudin 6* (*CLDN6*), a key component of tight junctions. *CLDN6* showed moderate or higher mRNA expression in eight of nine AT/RTs, with little to no expression in 114 of 115 other tumors. Average expression was 38-fold higher in AT/RTs vs. other samples. Immunohistochemical (IHC) staining of 33 tumor specimens found positive membrane staining in seven of seven AT/RTs, and was negative in 26 of 27 other brain tumor samples. Notably, none of the 16 medulloblastomas/primitive neuroectodermal tumors showed IHC staining for CLDN6. IHC staining results closely matched the level of mRNA expression detected by microarray. CLDN6 may be a useful positive marker to help further identify AT/RTs for diagnostic and treatment purposes.

BACKGROUND

Atypical teratoid/rhabdoid tumors (AT/RTs) are highly aggressive malignant central nervous system (CNS) tumors of early childhood. Prognosis is extremely poor, with median reported survival times ranging from 6 to 17 months (7, 8).

Historically, a subset of medulloblastomas diagnosed in children 2 years of age or younger was noted to behave extremely aggressively; careful studies prompted reclassification of some of these cases as a new tumor entity, AT/RT (29). AT/RTs display highly variable numbers of rhabdoid cells, defined as cells with eccentrically-placed nuclei with vesicular chromatin, prominent nucleoli, cytoplasmic eosinophilic globular inclusions, and well-defined cell borders (20). In addition, polyphenotypic immunohistochemical (IHC) expression is common, where mesenchymal, epithelial and/or neuronal components may be found within the same tumor. AT/RTs almost invariably show immunoreactivity for epithelial membrane antigen and vimentin, and usually also for smooth muscle actin (SMA); variable expression is seen for glial fibrillary acidic protein, neurofilament protein, synaptophysin (a neuronal marker) and keratins (20). Neither morphological nor IHC features of germ cells are identified, excluding consideration of teratoma or mixed teratomatous germ cell tumors. However, differential diagnosis of AT/RTs from other CNS tumors such as supratentorial primitive neuroectodermal tumors (PNETs), medulloblastomas, large cell medulloblastomas and choroid plexus carcinomas remains very difficult based on histopathology alone.

In the 1990s, it was observed that AT/RTs and malignant rhabdoid tumors of the kidneys and other soft tissues often demonstrate a loss of all or part of chromosome 22 (monosomy 22) (3, 30). It was subsequently discovered that deletion or mutation of the *INI1* gene (also known as SMARCB1, hSNF5, BAF47), found at chromosome 22q11.2, was a common characteristic of all of these rhabdoid tumors (4, 5, 35). INI1 is a component of the SWI/SNF complex that regulates transcriptional activity through chromatin remodeling (18). Subsequently, multiple studies have shown that a loss of INI1 protein expression caused by homozygous deletions or truncating mutations of *INI1* are associated with rhabdoid tumors; missense mutations that would result in dysfunctional INI1 protein but would retain protein staining are generally not seen (6, 16, 17). For this reason, loss of INI1 protein expression is a reliable indicator of loss of protein function, and consequently an

immunohistochemistry stain for INI1 is now often used for the diagnosis of AT/RTs. This stain shows the loss of INI1 in AT/RT tumor cell nuclei, whereas it is retained in cells of the vasculature and other CNS tumors, making this the first brain tumor in which the diagnosis is virtually defined by the absence of a single IHC marker. This immunostain is useful even when only a small section of tumor is available for analysis, as the absence of INI1 staining is generally seen in all AT/RT tumor cells, unlike the heterozygous immunophenotypic expression of epithelial, mesenchymal or neuronal markers in this tumor. Indeed, some authors have argued that loss of INI1 nuclear protein expression is the "gold standard" for diagnosis of AT/RT even in cases where only a small blue cell component is present by microscopy (12). Complicating the issue, however, is the fact that a small subset of tumors have been identified that display loss of INI1, but show atypical histopathological features for AT/RTs (6). There remains debate over how these tumors should be classified (11, 12). In addition, a small subset of tumors have been found that show classic histological AT/RT features, but retain INI1 staining, raising the possibility that a second locus might exist that can lead to AT/RT pathology (6, 9).

Many different treatment approaches to AT/RTs have been tried to date, including surgery, radiation and chemotherapy, alone or in combination. Survival times over 2 years have been uncommon with any of these strategies (see 28 for review). Either intense myeloablative chemotherapy (10) or sarcoma-based treatment regimens (40) have recently resulted in some successes. In addition, the development of targeted therapies is becoming increasingly prominent as a treatment approach for malignancies. However, for proper development and evaluation of new treatments, it is important that the tumors treated on any given regimen represent as homogeneous a group as possible. Thus, the ability to render diagnoses that reflect the biological underpinnings of the tumors in question continues to gain in importance.

With these issues in mind, we sought additional biological markers that might prove useful in the differential diagnosis of AT/RTs. Both gene expression microarray analysis and immunostaining of tumor tissue sections were conducted to evaluate mRNA and protein expression, respectively, in a large set of pediatric and adult CNS tumors, and selected pediatric sarcomas. Results were also compared with normal brain samples.

MATERIALS AND METHODS

Tumor specimens

All tumor specimens originated from patients who had received their surgical procedures at the University Hospital, Denver or The Children's Hospital, Denver between 1995 and 2008. Tumors were classified according to international guidelines as published in the 2007 World Health Organization (WHO) Classification of Tumors (20). All AT/RT samples were collected prior to initial treatment, as were most of the tumors within the collection with the exception of recurrent ependymomas and radiation-induced tumors. One specimen of normal choroid plexus tissue was also collected during tumor resection. All the specimen collection and subsequent processing were conducted in compliance with internal review board regulations (COMIRB #95–500).

To be eligible for this study, only AT/RTs and PNETs with classic morphological and IHC staining patterns were included, as defined by the WHO (20). Specifically, all AT/RTs possessed rhabdoid cells, at least focally, and all showed homogeneous loss of nuclear immunostaining for the INI1 (BAF47) protein. None of the classic medulloblastomas, large cell medulloblastomas or supratentorial PNETs showed loss of INI1 protein. We included seven choroid plexus papillomas (CPPs) and a single choroid plexus carcinoma (CPC) with retention of INI1 staining, but specifically did not assess controversial choroid plexus carcinomas with potentially overlapping features (37) or small blue cell tumors with loss of INI1 nuclear staining (12). The majority of AT/RTs has been assessed for presence or absence of monosomy 22 by fluorescence *in situ* hybridization (Table 1); specific *INI1* mutation status is not routinely performed at our institution and was not known for most cases.

Gene expression microarray analysis

To identify potential positive diagnostic markers relevant to AT/RTs, patient tumor samples were evaluated for gene expression using Affymetrix U133Plus2 GeneChip® microarrays (Affymetrix, Santa Clara, CA, USA), which include probes for all currently identified human genes. Samples for microarray analysis were col-

Table 1. Atypical teratoid/rhabdoid tumor (AT/RT) patient data.

Sample ID	Sex	Location	Chromosome 22 monosomy	Age at diagnosis (month)	Survival (month)	Died of disease?
3	Female	Posterior fossa	?	19	12	Yes
119	Male	Posterior fossa	Yes	11	6	Yes
370	Female	Posterior fossa	N	6	4	Yes
404	Male	Posterior fossa	Yes	5	7	Yes
413	Male	Posterior fossa	Yes	46	10	Yes
514	Male	Parietal/occipital lobes	No	33	16	Yes
515	Male	Frontal lobe	No	17	16	No
517	Male	Posterior fossa	Yes	24	16	No
605	Male	Frontal lobe	Yes	38	6	No

Characteristics of nine patients analyzed in this study with AT/RT diagnosis as determined both by typical histopathological features and loss of INI1 expression. Chromosome 22 monosomy was assessed by fluorescence *in situ* hybridization.

lected at the time of surgery and were either snap frozen and stored in liquid nitrogen, or immediately placed in RNAlater (Qiagen, Valencia, CA, USA) until further use. RNA was extracted from each sample using an RNeasy kit (Qiagen) or AllPrep DNA/RNA Mini kit (Qiagen) according to the manufacturer's directions. Five micrograms of RNA was then amplified and labeled using the Enzo BioArray™ HighYield™ RNA transcript labeling kit (Enzo Life Sciences, Farmingdale, NY, USA). The quality of the resulting RNA was verified using the Nano Assay Protocol for the 2100 Bioanalyzer (Agilent, Santa Clara, CA, USA). The prepared RNA was hybridized to HG-U133 Plus 2 GeneChips (Affymetrix), according to the manufacturer's instructions, as described previously (2).

A total of 124 pediatric and adult tumor samples and one pediatric normal choroid plexus sample were analyzed by microarray. The samples included nine AT/RTs, as well as glioblastomas, medulloblastomas, large cell medulloblastomas, ependymomas, pilocytic astrocytomas, Ewing's sarcomas, rhabdomyosarcomas, meningiomas, CPPs, radiation-induced tumors and others (see Table 2). All the nine AT/RTs displayed both typical histopathological features associated with AT/RTs as defined in WHO (20) and a lack of INI1 staining. The frequent loss of chromosome 22, young age at diagnosis and short survival times seen in our AT/RT patients (Table 1) are typical of what has been reported in the literature for this type of tumor (see 28 for review).

In addition, publicly available CEL file data for 66 normal brain specimens from 10 post-mortem donors processed on HG-U133 Plus 2 GeneChips (Affymetrix) were downloaded from GEO (http://www.ncbi.nlm.nih.gov/geo/; accession GSE3526) for comparison with the tumor specimen data.

Data analysis was done using the R programming language (http://www.r-project.org/). Microarray data from both the processed tumor samples and the GEO GSE3526 dataset were background corrected and normalized using the gcRMA algorithm (36), resulting in log 2 expression values. Differential expression of genes was determined using limma, which employs an empirical Bayes approach to calculate a moderated *t*-statistic (31). For input to hierarchical clustering, gene expression data were pre-filtered to eliminate genes not expressed in any samples, or those that showed only limited variability across samples. The hierarchical clustering used distances based on Spearman correlations as input to an agglomerative algorithm using complete linkage, as implemented in the hclust package. All packages listed above are open-source R software available online through the Bioconductor project website (http://www.bioconductor.org).

Quantitative real-time polymerase chain reaction (PCR)

Gene copy number amplification was examined using quantitative real-time PCR performed on a Chromo4 Real Time Detector

Table 2. Samples analyzed by microarray.

Category	Tumor sample diagnosis	Abbreviation	Number of samples
AT/RT	Atypical teratoid/rhabdoid tumor	ATRT	9
CPC/CPP	Choroid plexus carcinoma	CPC	1
CPC/CPP	Choroid plexus papilloma	CPP	4
EPN	Ependymoma	EPN	27
HGG	Radiation-induced glioblastoma	RIG	5
HGG	Glioblastoma (pediatric)	GBM	13
HGG	Glioblastoma (adult)	GBM	6
HGG	High grade glioma	HGG	1
HGG	Oligodendroglioma (adult)	ODG	1
LGA	Ganglioglioma	GG	1
LGA	Pilocytic astrocytoma	PA	9
LGA	Pilomyxoid astrocytoma	PMA	3
LGA	Pleomorphic xanthoastrocytoma	PXA	1
MEN	Meningioma (7 adults)	MEN	8
MEN	Radiation-induced meningioma (adult)	RIM	5
MPNST	Malignant peripheral nerve sheath tumor	MPNST	3
PNET/MED	Large cell medulloblastoma	LARGE	4
PNET/MED	Classic medulloblastoma	MED	8
PNET/MED	Primitive neuroectodermal tumors (supratentorial)	PNET	3
Sarcoma	Malignant ectomesenchymoma	MEM	1
Sarcoma	Ewing sarcoma	EWS	2
Sarcoma	Radiation-induced sarcoma (adult)	RIS	1
Sarcoma	Rhabdomyosarcoma	RMS	8
	Total tumor samples		124
	Normal samples		
	Choroid plexus	CP	1
	Normal brain (adult; GEO series GSE3526)	NORM	66
	Total normal brain samples		67

Tumor samples are from pediatric cases unless indicated otherwise. Individual diagnoses are grouped together to form more general categories of similar tumor types that are used in Figure 1.

(Bio-Rad, Hercules, CA, USA). Power SYBR Green PCR Master Mix (Applied Biosystems, Foster City, CA, USA) was used for detection chemistry. Approximately 35 ng of DNA, extracted from tumor samples using an AllPrep DNA/RNA Mini kit (Qiagen) according to the manufacturer's directions was used in each reaction. PUS7L was used as a reference gene because of its extremely stable mRNA expression in all samples, and no previous indications of amplification in cancer. Primers were designed to include at least part of an intron, to ensure there was no amplification from any contaminating mRNA. Primer sequences were: *PUS7L* forward: 5′-GTTTCAGAGGATGCTAAAGGCACACTTTC-3′; *PUS7L* reverse: 5′-GATACAACCTTCCTCGGTCATGCC-3′; *CLDN6* forward: 5′-CTTAAACTCAGGGCTAGAATTGAACC-3′; and *CLDN6* reverse: 5′-AACCTATACAATGACAGTCCA AGGC-3′. Conditions for amplification were as follows: one cycle of 95°C for 2 minutes; followed by 40 cycles of 95°C for 30 s; 58°C for 30 s; and 70°C for 30 s. Threshold cycle numbers were obtained using the Bio-Rad software. PCRs for each primer set/tumor combination were performed in quadruplicate and threshold cycle numbers were averaged. Copy number changes per haploid genome were calculated using the $2^{-\Delta\Delta Ct}$ method.

Immunoblotting

Total protein lysates were prepared from tumor samples by homogenization of approximately 50 mg of specimen in 500 µL of lysis buffer (50 mM HEPES, pH 7.5; 150 mM NaCl; 10 mM ethylenediaminetetraacetic acid; 10% glycerol; 1% Triton X-100; 1 mM sodium vanadate; and 1 mM sodium molybdate) with a complete Mini ProteaseInhibitor Cocktail (Roche, Indianapolis, IN, USA) using a PowerGen Rotor-Stator homogenizer (Fischer Scientific, Pittsburgh, PA, USA). Fifty micrograms of the resulting protein lysates were incubated with loading dye, separated on precast 4% to 15% Criterion sodiumdodecyl sulfate Tris-glycine gel (Bio-Rad, San Diego, CA, USA) and transferred to a polyvinylidene difluoride membrane (Millipore, Billerica, MA, USA). Membranes were incubated with the appropriate antibodies and antibody binding was visualized by enhanced chemiluminescence (Perkin Elmer, Boston, MA, USA) exposure to X-Omat Blue XB-1 imaging film (Eastman Kodak, Rochester, NY, USA).

Immunohistochemistry

Immunohistochemistry was performed on paraffin-embedded tumor tissue sections. Slides were de-paraffinized, and antigen retrieval was performed using Ph9 Borg Buffer (BioCare Medical, Concord, CA, USA) for 15 minutes at 93°C followed by a 20-minute cool down. Subsequent steps were performed using the EnVision-HRP kit (Dako, Glostrup, Denmark) on a Dako autostainer according to the standard protocol. Incubation with primary antibody was performed for 2 h.

Antibodies

Primary antibodies used for Western blotting included rabbit polyclonal anti-claudin 6 1:1000 (01-8865; American Research Products, Belmont, MA, USA); mouse monoclonal anti-BAF47 (INI1) 1:1000 (612110, BD Transduction Laboratories, San Jose, CA, USA); and goat polyclonal anti-A-actin 1:3000 (sc-1616; Santa Cruz Biotechnology, Santa Cruz, CA, USA). For immunohistochemistry, the same claudin 6 antibody was utilized at a dilution of 1:66.

RESULTS

AT/RTs, but not most other brain tumors or normal brain, express moderate to high levels of claudin 6 mRNA by microarray

Analysis of the Affymetrix gene expression microarray data, which measures gene transcript levels (mRNA), showed that there were multiple genes with statistically significant differences at a false discovery rate of $P < 0.05$ when AT/RTs were compared with tumors in each of the other categories. To hone in on the genes with greatest potential for diagnostic utility, we focused on those genes that were expressed in moderate or high levels in AT/RTs, but not in other confounding tumor types. Thus, criteria for gene selection were defined as: (i) the gene should be expressed at moderate or higher levels in almost all AT/RTs (ie, high sensitivity as a positive marker); (ii) the gene should show little to no expression in most other tumors (ie, high specificity); (iii) genes showing fewer samples with overlap in expression between AT/RTs and other tumors were preferable; and (iv) protein expression should follow a similar pattern. After additional analysis, the three genes that best met these criteria were *claudin 6* (*CLDN6*), *ubiquitin specific peptidase 44* (*USP44*) and *sal-like 4* (*SALL4*), as shown in Figure 1.

Although *USP44* was expressed at moderate to high levels in AT/RTs, tumors in the PNET/MED category did show some overlap with AT/RTs (Figure 1A), excluding this gene from further consideration based on specificity criteria. *SALL4* (Figure 1B) showed fewer overlaps than *USP44*, but these overlaps were primarily among the PNET/MED category, one of the diagnostically most confounding tumor types. Therefore, *SALL4* was also excluded from further study. On the other hand, eight of nine AT/RTs showed moderate to strong expression of *CLDN6*, whereas all samples within the PNET/MED category showed little to no expression of this gene (Figure 1C). In fact, of the 115 non-AT/RT tumors and 67 normal samples, only one—a CPP—showed more than a minimal level of expression of *CLDN6*. The mean expression for the nine AT/RTs was 38-fold higher than the mean expression for all other tumors and normal samples; this difference was highly significant at $P < 2.0 \times 10^{-66}$ using a two-tailed *t*-test. Gene expression values, expressed on a log 2 scale ranging roughly from 0 to 16, showed an overall mean expression for all genes of 4.9. As measured on this scale, the mean for *CLDN6* expression in AT/RTs was 8.0, indicating above average expression, whereas the mean in all other tumors, as well as in the normal samples, for *CLDN6* was 2.8, indicating extremely low to no expression of *CLDN6* in either of these groups. Thus, *CLDN6* mRNA levels were a positive marker for AT/RTs with a high degree of sensitivity and specificity.

To evaluate whether high *CLDN6* levels might be due to gene amplification, quantitative real-time PCR (qPCR) was performed using DNA from tumor samples showing strong *CLDN6* expression. *Pseudouridylate synthase 7 homolog* (*PUS7L*) was chosen as a reference gene because of its extremely consistent expression across all study samples and no known links with cancer, therefore making it unlikely that it was amplified in any of the samples. The

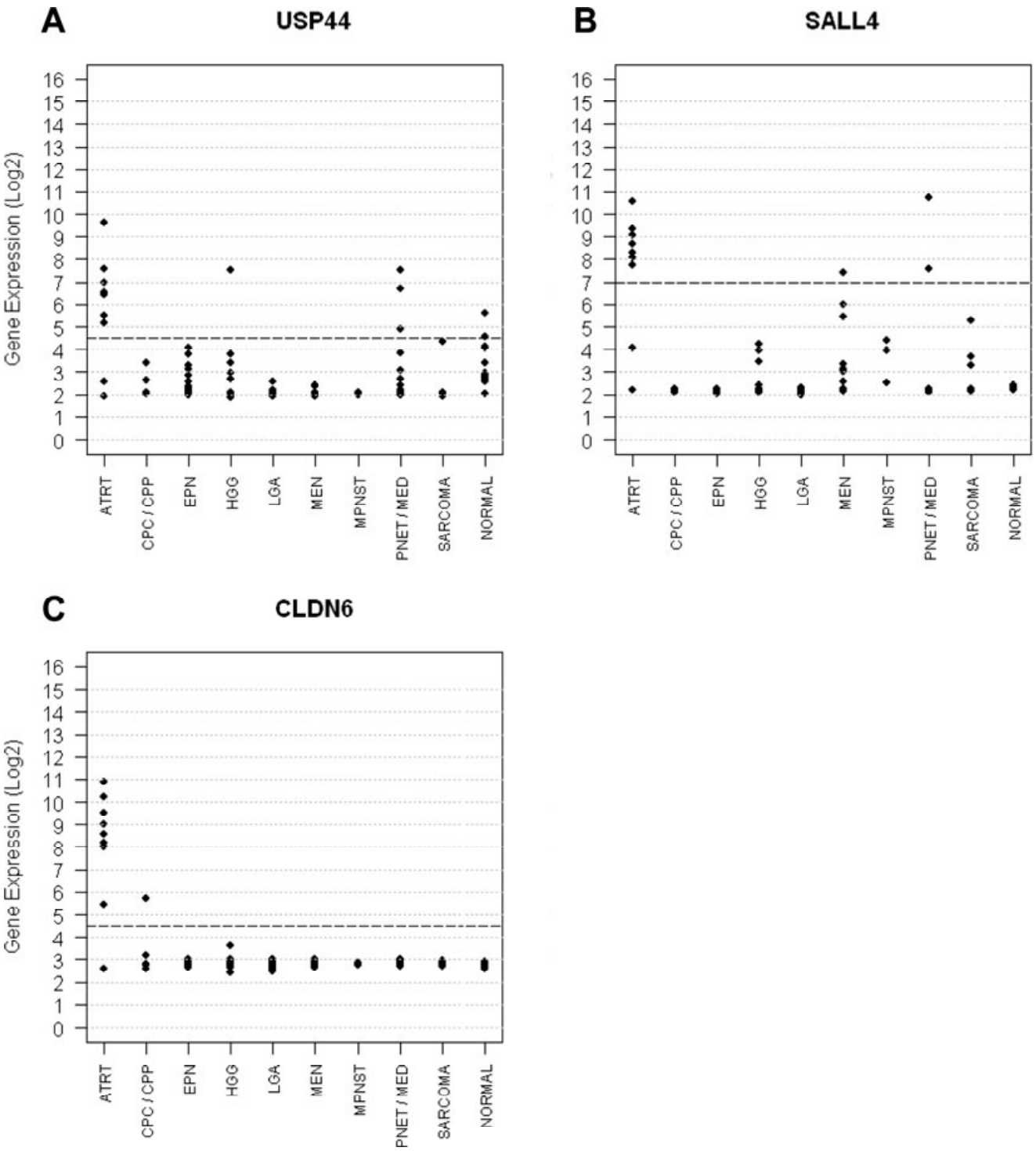

Figure 1. *mRNA Expression of selected genes as assessed by microarray. Dot plots of normalized log 2 gene expression as measured by Affymetrix HG U133 Plus 2 Gene Chip microarray for selected genes, by tumor diagnostic group.* For specific diagnoses and counts of tumors included in each diagnostic group, see Table 2. **A.** *Ubiquitin specific peptidase 44* (*USP44*). **B.** *Sal-like 4* (*SALL4*). **C.** *Claudin 6* (*CLDN6*). Abbreviations: AT/RT = atypical teratoid/rhabdoid tumor; CPC/CPP = choroid plexus carcinoma/choroid plexus papilloma; EPN = ependymoma; HGG = High-grade glioma; LGA = low-grade astrocytoma; MEN = meningioma; MPNST = malignant peripheral nerve sheath tumor; PNET/MED = primitive neuroectodermal and medulloblastoma tumors.

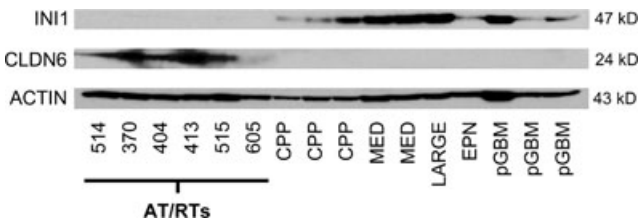

Figure 2. *Expression of* INI1 *and* claudin 6 (CLDN6) *in tumor samples as assessed by Western blot.* Equal amounts of tumor sample lysates were analyzed by Western blot for the proteins indicated. Beta-actin was used as a loading control. Abbreviations: AT/RT = atypical teratoid/rhabdoid tumor; CPP = choroid plexus papilloma; EPN = ependymoma; LARGE = large-cell medulloblastoma; MED = classic medulloblastoma; pGBM = pediatric glioblastoma.

resulting haploid gene copy numbers for *CLDN6*, which ranged from 0.7 to 1.5, did not indicate any amplification of the *CLDN6* gene in these samples.

AT/RTs, but not most other brain tumors or normal brain, express CLDN6 protein by Western blot analyses

Next, protein expression was analyzed by Western blotting using whole cell tumor lysates of a subset of AT/RTs and other tumors. Lack of INI1 expression in AT/RTs was confirmed on Western blotting using a BAF47 antibody. As expected, INI1 expression was absent in AT/RTs, but present in other tumors. Presence of the CLDN6 protein was examined using a commercially available antibody. CLDN6 protein expression showed the opposite pattern from INI1, with strong expression seen in the AT/RTs, but no expression observed for other tumors (Figure 2).

AT/RTs, but not most other brain tumors or normal brain, express CLDN6 protein by immunohistochemistry (IHC)

To verify that CLDN6 expression occurred in tumor cells rather than in other cells such as those of the vasculature, IHC was performed on tumor samples using the same commercially-available CLDN6 antibody that was utilized for Western blotting. All samples were assessed for positive or negative staining by the neuropathologist on the study (B. K. Kleinschmidt-DeMasters). Seven AT/RT samples were available for IHC staining. IHC was performed on these seven AT/RTs as well as 27 additional CNS tumors, for a total of 34 samples.

Results of IHC staining are summarized in Table 3. Positive immunoreactivity for CLDN6 was seen in seven of seven AT/RTs. One CPP also showed positive immunoreactivity, whereas the remaining 26 of 27 non-AT/RTs showed negative immunoreactivity. Endothelial cells and other non-tumor tissue (eg, adjacent brain tissue) within the resection specimens also showed negative immunoreactivity for CLDN6.

Examples of IHC staining are shown in Figure 3. Several features were consistently observed in all of the AT/RT cases. First, there was a distinct tendency for the CLDN6 immunostaining to occur in clusters of contiguous cells more often than in single, individual, widely dispersed cells. The extent of immunostaining ranged from being widespread throughout most of a low power microscopic field (Figure 3A, case 404), to zonal (Figure 3B, case 514), to, in one case, extremely focal (Figure 3C, case 605). In this latter example (case 605), staining still appeared to be within a cluster of cells (Figure 3C). Case 605 was significant in that it possessed the largest volume of small blue, undifferentiated cells in the tumor and most of the tumor fields were devoid of CLDN6 immunostaining.

Second, higher power inspection revealed that the positive immunostaining tended to preferentially be in cells with a larger cytoplasmic volume and in rhabdoid cells (Figure 3D, case 517 illustrated). Nevertheless, in some instances CLDN6 immunostaining could be identified in cells without obvious rhabdoid features (Figure 3E, case 605 illustrated); interestingly, these positively immunostaining cells often possessed nuclear and cytoplasmic features nearly identical to their negatively immunostaining neighbors. Conversely, not all large rhabdoid cells were immunoreactive (Figure 3F, arrow, case 605 illustrated).

Third, immunostaining for CLDN6 occurred in a membranous pattern (Figure 3G, case 515 illustrated; Figure 3H, case 517 illustrated), in contrast to the nuclear staining of INI1 (BAF47). Nuclear staining of CLDN6 was not observed.

All classic medulloblastomas ($n = 10$), large cell medulloblastomas ($n = 3$), CNS PNETs from supratentorial sites ($n = 3$) and glioblastomas ($n = 3$) were entirely negative for CLDN6, without even isolated cells with membranous immunoreactivity (Figure 3I). Indeed, the only non-AT/RT sample that possessed significant immunostaining for CLDN6 was a single pediatric choroid plexus papilloma. This CPP (which also showed moderate levels of *CLDN6* mRNA gene expression on microarray) showed patchy zones of immunoreactivity in several areas of the tumor (Figure 4A). Staining was confined to membranes at the lumenal and lateral surfaces of the cells (Figure 4A). Matched sections of this same CPP immunostained for INI1 (BAF47) showed complete

Table 3. Immunohistochemical staining results for CLDN6. Thirty-four samples were evaluated using immunohistochemical (IHC) staining for expression of CLDN6 protein. Positive/negative staining was judged by a pathologist blind to the tumor diagnosis. Results are shown grouped by type of tumor. Abbreviations: AT/RT = atypical teratoid/rhabdoid tumor; CPC = choroid plexus carcinoma; CPP = choroid plexus papilloma; LARGE = medulloblastoma, large cell variant; MED = classic medulloblastoma; PNET = primitive neuroectodermal tumor (supratentorial); GBM = glioblastoma.

Diagnosis	Number of samples tested	Results
AT/RT	7	7 positive (1 of these only in a few very limited areas)
CPC	1	All negative
CPP	7	1 positive, 6 negative
LARGE	3	All negative
MED (pediatric)	6	All negative
MED (adult)	4	All negative
PNET	3	All negative
GBM (pediatric)	2	All negative
GBM (adult)	1	All negative

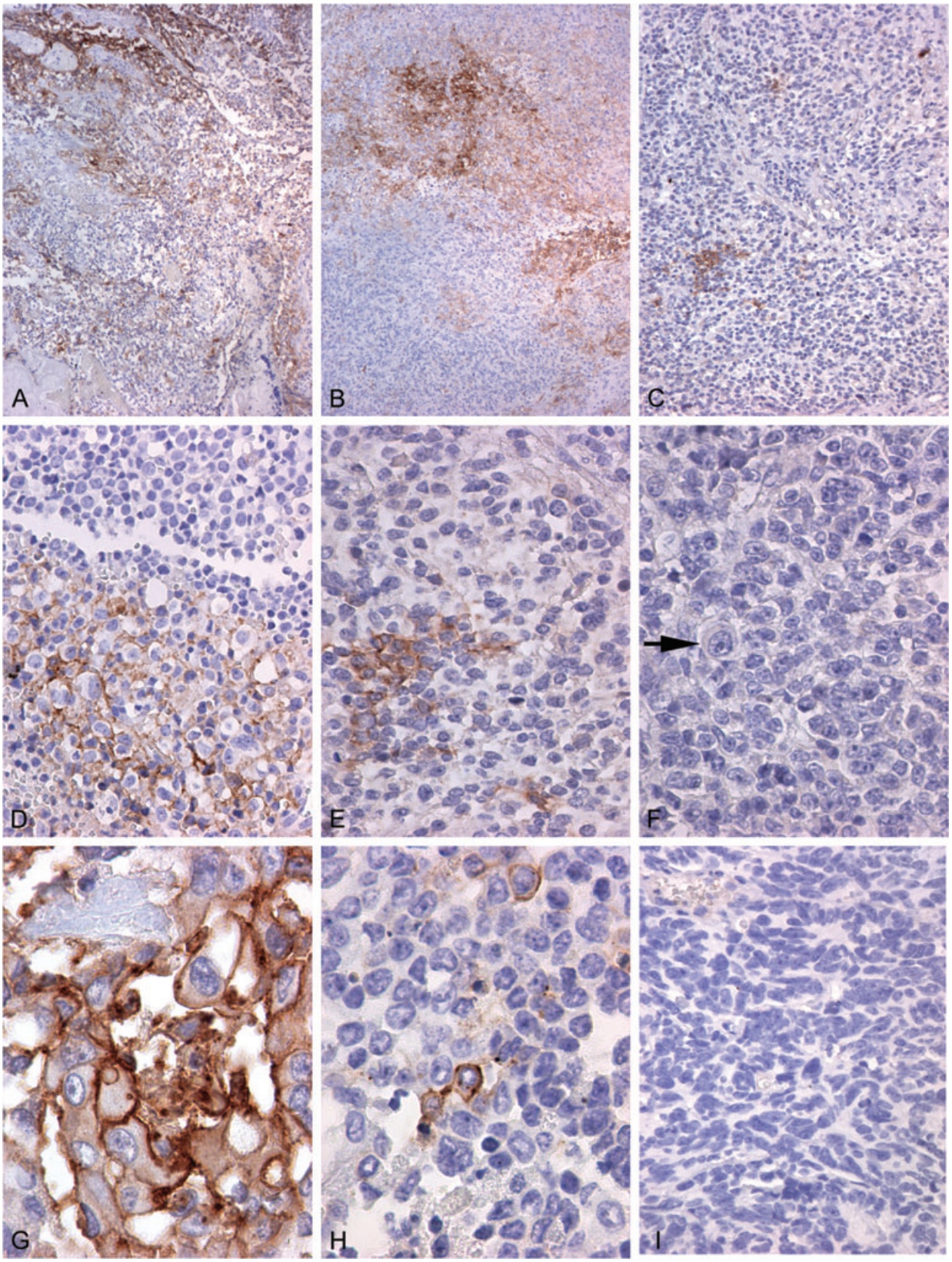

Brain Pathology **20** (2010) 140–150

Figure 3. CLDN6 *immunostaining in pediatric brain tumors. Photomicrographs illustrating immunostaining results for* claudin 6 (CLDN6), *with light hematoxylin counterstain.* **A.** Low-power view illustrates that some atypical teratoid/rhabdoid tumors (AT/RTs) manifested diffuse immunostaining for CLDN6 throughout the tumor. AT/RT, case 404, original magnification 100×. **B.** Low-power view illustrates that other AT/RTs had immunostaining for CLDN6 in large islands of cohesive cells. AT/RT, case 514, original magnification 100×. **C.** Low-power view illustrates that one AT/RT case possessed only small groups of cells that were immunoreactive for CLDN6 in a field of otherwise negatively staining cells. AT/RT, case 605, original magnification 100×. **D.** Medium-power view illustrates that positive immunostaining occurred more often in rhabdoid cells and in cells with larger cytoplasmic volume. AT/RT, case 517, original magnification 400×. **E.** Medium-power view illustrates that CLDN6 immunostaining could be found in cells without obvious rhabdoid features. AT/RT, case 605, original magnification 600×. **F.** Medium-power view shows absence of CLDN6 immunostaining in some rhabdoid cells (arrow). AT/RT, case 605, original magnification 600×. **G.** High-power view highlights the strong membranous pattern of CLDN6 staining in AT/RTs. AT/RT, case 515, original magnification 1000×. **H.** High-power view emphasizes that even in immunoreactive cells with smaller cytoplasmic volume the pattern of immunostaining for CLDN6 remained membranous. AT/RT, case 517, original magnification 1000×. **I.** Medium-power view illustrates that almost all non-AT/RT cases had negative immunoreactivity for CLDN6. Large cell medulloblastoma, original magnification 400×.

retention of INI1 nuclear protein (Figure 4B). Another CPP in a pediatric patient showed less than a half dozen positive cells; not surprisingly, this pediatric CPP showed no elevated *CLDN6* expression by microarray. The remaining five CPPs, two pediatric and three adult, and a classic CPC in a pediatric patient were completely negative by IHC (and microarray).

CLDN6 mRNA expression levels show good correspondence with immunohistochemistry results

Fourteen samples in this study were available for assessment of both mRNA gene expression by microarray and protein expression by IHC; these consisted of seven AT/RTs and seven other tumors. The level of mRNA expression measured by microarray corresponded well with the extent of CLDN6 protein visualized by IHC (Table 4).

Specifically, the microarray gene expression values of the 14 samples that were evaluated by both gene expression microarray and by IHC fell into two clearly separated ranges: seven samples showed moderate to strong mRNA expression of *CLDN6*, with values in the range of 5.4 to 10.9 (log 2). The other seven samples showed little to no expression of *CLDN6*, with values in the range of 2.7 to 2.9. All samples that showed moderate to strong expression of *CLDN6* mRNA by microarray also showed positive immunoreactivity to CLDN6 as evaluated by IHC. Of the seven samples that showed little to no expression of CLDN6 mRNA by microarray, six were immunonegative for CLDN6 as evaluated by IHC. The seventh, an AT/RT (case 605), showed very little *CLDN6* mRNA expression (2.6), but did show positive immunoreactivity for CLDN6 in a few focal areas.

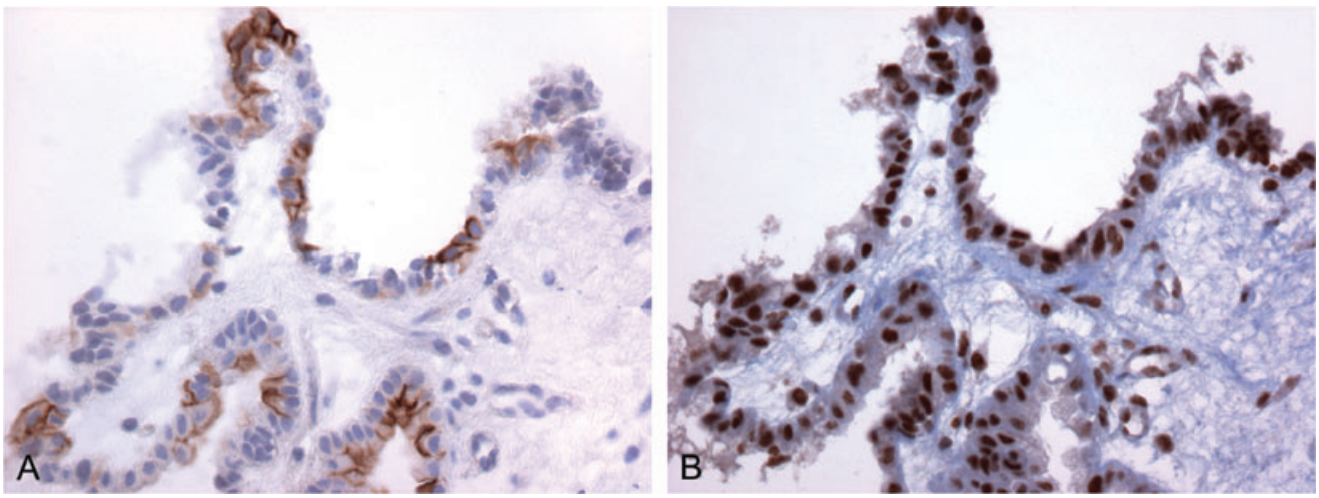

Figure 4. CLDN6 *and* INI1 *protein expression in choroid plexus papilloma (CPP) case 451. Photomicrographs illustrating immunostaining results for* claudin 6 (CLDN6) *and* INI1, *with light hematoxylin counterstain.* **A.** Medium-power view illustrates that a few areas of positive immunoreactivity for CLDN6 could be found in one choroid plexus papilloma. Staining is limited to the membranes at the lumenal and lateral cell surfaces. CPP, case 451, original magnification 400×. **B.** Medium-power view from the same tumor area as seen in Figure 4A, immunostained for INI1 (BAF47), showing complete retention of INI1 nuclear protein. CPP, case 451, original magnification 400×.

Table 4. Comparison of mRNA expression and IHC results. Comparison of microarray gene expression values (log 2) and IHC results for samples which were evaluated by both methods. Results are in descending order of mRNA gene expression. Abbreviations: AT/RT = atypical teratoid/rhabdoid tumor; CPC = choroid plexus carcinoma; CPP = choroid plexus papilloma; IHC = immunohistochemistry; LARGE = medulloblastoma, large cell variant; MED = classic medulloblastoma; PNET = primitive neuroectodermal tumor (supratentorial).

Tumor type	Sample ID	mRNA expression (log 2)	IHC results
AT/RT	404	10.9	Positive
AT/RT	370	10.2	Positive
AT/RT	413	9.5	Positive
AT/RT	514	9.0	Positive
AT/RT	517	8.2	Positive
CPP	451	5.7	Positive
AT/RT	515	5.4	Positive
LARGE	401	2.9	Negative
MED	330	2.9	Negative
MED	254	2.8	Negative
PNET	383	2.8	Negative
PNET	536	2.8	Negative
CPC	233	2.7	Negative
AT/RT	605	2.6	Positive in a few limited areas

Diagnostic groups cluster closely together based on gene expression pattern, however, AT/RT 605 does not cluster with the other AT/RTs

Brain tumor diagnosis is based primarily on histopathological features. An additional informative approach that can be employed to define tumor groups is to apply hierarchical clustering to gene expression microarray data. Hierarchical clustering results in a tree structure (dendrogram) that groups samples with similar gene expression together on branches; this clustering has been shown to be relevant to diagnostic classification (26). To further evaluate the tumor samples used in this study, hierarchical clustering was performed with the same gene expression microarray data used for initial identification of *CLDN6* (Table 2).

The clustering results showed that most tumors in a diagnostic category were placed on close branches of the dendrogram, indicating that they shared similar patterns of gene expression. The eight AT/RTs that showed moderate to strong *CLDN6* expression were consistent with this pattern, clustering together in one group. However, AT/RT case 605, despite the presence of rhabdoid cells, loss of INI1 protein and monosomy 22 in this tumor, did not cluster with the other eight AT/RTs but instead clustered with the "astrocytic tumors" group, comprised mostly of glioblastomas, pilocytic and pilomyxoid astrocytomas. This was the same AT/RT case that showed only minimal to no *CLDN6* expression as measured by microarray, even though extremely focal positive immunoreactivity for CLDN6 was seen by IHC (see Figure 3C). Failure to cluster with the other AT/RTs indicates that case 605 displayed a more divergent pattern of gene expression, beyond that of just *CLDN6* expression alone, from the other AT/RTs.

DISCUSSION

AT/RTs have been recognized as a separate diagnostic entity for only the past decade. Histopathologically, this tumor is defined by its polyphenotypic expression and the presence of rhabdoid cells. Additionally, it was documented in the 1990s that these tumors exhibit a loss of INI1 protein, whereas most other brain tumors do not (4, 16, 35). INI1 loss has also been reported in other non-CNS tumors, including renal rhabdoid tumors and soft-tissue rhabdoid tumors (5), which are closely related to AT/RTs, as well as unrelated tumor types such as familial schwannomas (25) and epithelioid sarcomas (22). Because of the difficulty of reliably distinguishing between AT/RTs and other tumors based solely on histopathological criteria, loss of INI1 nuclear protein is often used as a definitive diagnostic marker. AT/RTs are currently the only CNS tumor to be virtually defined by the absence of a single protein. However, debate remains as to how to classify CNS tumors that lack INI1 but do not show histopathological features of AT/RTs, as well as tumors that histopathologically appear to be AT/RTs but show retention of INI1 staining. Given the poor survival associated with past treatment regimens, the development and testing of new treatments, such as the use of targeted therapeutic agents or sarcoma-based therapies, is of utmost priority. Identification of useful treatments improves as understanding of the underlying biological processes associated with a tumor entity improves. Accurate analysis of treatment outcomes also hinges on consistent diagnostic classification. Thus, the relationship between the diagnostic category and the lack of INI1 takes on increased significance. Continued search for identification of additional, positive markers associated with AT/RTs as an aid to differential diagnosis is of value.

In this study, nine AT/RT tumor samples that met the 2007 WHO histopathological guidelines (20) and showed INI1 protein loss were compared with 104 other CNS tumors and 11 sarcomas from both pediatric and adult patients, as well as 67 normal brain samples, for gene expression as measured by Affymetrix microarray. Based on these data, *CLDN6* was identified as a gene that showed moderate to strong mRNA expression in eight of nine AT/RTs, but little to no expression in 114 of 115 other tumors and in all of the normal brain tissue samples (including one normal choroid plexus sample).

Subsequent evaluation by IHC of seven AT/RT tumor samples and 27 non-AT/RT tumor samples showed positive immunoreactivity for CLDN6 in all of the AT/RT samples, whereas 26 of 27 non-AT/RT samples were negative. Only one non-AT/RT sample, a choroid plexus papilloma, showed positive immunoreactivity for CLDN6. This was also the only non-AT/RT sample to show higher than minimal amounts of *CLDN6* mRNA expression as measured by microarray. These results show that *CLDN6* is expressed by most AT/RTs, but not by most other brain tumors, and thus may be a useful aid in identification and study of pediatric brain tumors.

Strengths of this study are:(i) CLDN6 by IHC shows high sensitivity and specificity for AT/RTs and not other tumor types; (ii) strong concordance was found between level of *CLDN6* mRNA expression and IHC results; (iii) immunostaining can be achieved with readily-accessible, commercially available antibody to CLDN6; and (iv) CLDN6 immunostaining reveals positive cells within a tumor that are not obviously rhabdoid cells based on morphological features alone.

Potential weaknesses of this study are: (i) not all cells within an AT/RT are immunoreactive, leading to the problem of sampling error, perhaps especially for AT/RTs with large volumes of PNET-like cells; and (ii) an occasional CPP showed immunoreactivity for CLDN6. Classic CPP is unlikely to be morphologically mistaken for an AT/RT and the example in our cohort retained strong nuclear INI1 (BAF47) immunoreactivity, suggesting that positive CLDN6 immunostaining is not dependent on INI1 loss. If CLDN6 is utilized for diagnostic purposes, we envision that it would be used as an adjunct to, not a replacement for, INI1 (BAF47) immunostaining. CLDN6 immunostaining could potentially add an additional degree of confidence and an additional piece of supporting data for the diagnosis of AT/RTs.

Whether positive immunoreactivity for CLDN6 in AT/RTs additionally hints at histogenesis is unclear. *CLDN6* is a member of the claudin family of genes, which consist of over 20 members in humans, and is a critical component of tight junctions between cells. Tight junctions are situated on cell membranes, and our IHC analysis showed that, when present, CLDN6 was expressed specifically in tumor cell membranes in all tumors in our study. In mice, expression of *CLDN6* has been reported in normal epithelial tissues of the tongue, skin, stomach and breast in neonates (33) and in neonatal, but not adult, mouse and rat kidney (1, 39). Onset of expression of *CLDN6* has been shown to correlate with the development of epithelial cells from mouse embryonic cells, and has been found to be one of the earliest markers of cells committed to epithelial fate, along with keratin 8 (34). Similarly, a study using publicly available SAGE data for 266 normal and malignant human tissues found that *CLDN6* was primarily expressed in stem cells (14). Publicly available Affymetrix HG U133 Plus2 GeneChip microarray data (http://www.ncbi.nlm.nih.gov/geo/; accessions GSE7234 and GSE7896; data not shown) also show very high expression of *CLDN6* in human embryonic stem cell lines—similar or higher to that seen in our AT/RT tumors. These data underscore the role of this gene in early development and are of interest given the embryonic nature of AT/RT tumors, and the occurrence of AT/RTs primarily in very young children. Abnormal expression of claudin genes has been previously reported in various cancers (see 24, 32 for reviews). *CLDN6*, specifically, has been found to be lower in breast cancer vs. normal mammary tissue in humans and rats (27). It remains for future studies to determine what biological role the expression of *CLDN6* may play in the context of AT/RTs.

INI1 is a component of the multi-protein SWI/SNF complex. SWI/SNF is an adenosine triphosphate-dependent chromatin remodeling complex that is involved in both activation and repression of target genes. Numerous studies altering the expression of INI1 and measuring the resulting changes in gene expression have been performed (15, 19, 21, 23, 38). None of these studies has reported changes in *CLDN6* expression as a consequence of INI1 expression or inhibition. Therefore, it seems possible that expression of *CLDN6* in AT/RTs is an indirect effect of INI1 absence. As noted earlier, normal *CLDN6* expression appears to occur primarily in fetal and neonatal development, but does not appear present in most normal adult tissues. Therefore, it may be that expression of *CLDN6* in AT/RTs represents either the failure of a developmental program to be effectively turned off or its subsequent reinitiation upon INI1 loss. As INI1 expression has been shown to affect expression of many cell signaling components, in addition to cell-cycle and checkpoint control genes (15, 19, 21, 23, 38), this is a plausible connection. Developmental and molecular biology studies will be needed to understand the factors that affect *CLDN6* expression.

There were two examples in our study where CLDN6 expression and AT/RT diagnosis were discordant. The first was a tumor that met the criteria for AT/RT in every way, but showed large areas with small blue cells; IHC identified CLDN6 immunostaining in the tumor albeit very focally, although microarray analysis values indicated little to no expression of mRNA. Conceivably, sampling error in the piece blindly selected for mRNA analysis may have contributed to the very low microarray expression value despite the very focally positive IHC finding. The other discordance was in one CPP from a 4-month-old patient; however, the six other CPPs examined, including two other patients of similar age, were negative for CLDN6, as was the CPC. Perhaps the viewpoint offered by Bourdeaut *et al* (6) and also noted by others (11, 37) that "hSNF5/INI1-deficient tumours and rhabdoid tumours are convergent but not fully overlapping entities" should continue to be explored. It should be noted that thus far CLDN6 has not been identified as a signature marker for choroid plexus lesions on microarray studies (13), but may be a target for future investigations.

This research has only looked at rhaboid tumors occuring in the CNS; however, rhabdoid tumors also are known to occur outside of the CNS, most frequently in the kidney. A next step will be to examine non-CNS rhabdoid tumors for expression of CLDN6. Given that CLDN6 expression has been observed in normal neonatal rodent kidney (1, 39) it will be important to also include normal kidney tissue and other non-rhabdoid kidney tumors, and to cover a spectrum of patient ages. Studies are currently underway in our laboratories in this area.

In conclusion, CLDN6 immunostaining has the potential to be a useful adjunctive marker for AT/RTs, especially when used in concert with INI1 (BAF47) immunostaining. The availability of a commercial antibody for this gene, and the high fidelity seen between mRNA and protein expression in all samples examined, are additional attributes that contribute to CLDN6 as a potentially useful tool in achieving uniform tumor diagnosis and ultimately, formulation of uniform patient cohorts for treatment regimens. Determination of whether CLDN6 expression is fundamental to tumorigenesis of AT/RTs awaits further studies.

ACKNOWLEDGMENTS

We would like to thank the Morgan Adams Foundation and the Sean's Hope Foundation for financial support of this project.

REFERENCES

1. Abuazza G, Becker A, Williams SS, Chakravarty S, Truong HT, Lin F, Baum M (2006) Claudins 6, 9, and 13 are developmentally expressed renal tight junction proteins. *Am J Physiol Renal Physiol* **291**:F1132–F1141.
2. Addo-Yobo SO, Straessle J, Anwar A, Donson AM, Kleinschmidt-Demasters BK, Foreman NK (2006) Paired overexpression of ErbB3 and Sox 10 in pilocytic astrocytoma. *J Neuropathol Exp Neurol* **65**:769–775.
3. Biegel JA, Rorke LB, Packer RJ, Emanuel BS (1990) Monosomy 22 in rhabdoid or atypical teratoid tumors of the brain. *J Neurosurg* **73**:710–714.

4. Biegel JA, Zhou JY, Rorke LB, Stenstrom C, Wainwright LM, Fogelgren B (1999) Germ-line and acquired mutations of INI1 in atypical teratoid and rhabdoid tumors. *Cancer Res* **59**:74–79.
5. Biegel JA, Tan L, Zhang F, Wainwright L, Russo P, Rorke LB (2002) Alterations of the hSNF5/INI1 gene in central nervous system atypical teratoid/rhabdoid tumors and renal and extrarenal rhabdoid tumors. *Clin Cancer Res* **8**:3461–3467.
6. Bourdeaut F, Fréneaux P, Thuille B, Lellouch-Tubiana A, Nicolas A, Couturier J *et al* (2007) hSNF5/INI1-deficient tumours and rhabdoid tumours are convergent but not fully overlapping entities. *J Pathol* **211**:323–330.
7. Burger PC, Yu IT, Tihan T, Friedman HS, Strother DR, Kepner JL *et al* (1998) Atypical teratoid/rhabdoid tumor of the central nervous system: a highly malignant tumor of infancy and childhood frequently mistaken for medulloblastoma: a Pediatric Oncology Group study. *Am J Surg Pathol* **22**:1083–1092.
8. Chen ML, McComb JG, Krieger MD (2005) Atypical teratoid/rhabdoid tumors of the central nervous system: management and outcomes. *Neurosurg Focus* **18**:E8.
9. Frühwald MC, Hasselblatt M, Wirth S, Köhler G, Schneppenheim R, Subero JI *et al* (2006) Non-linkage of familial rhabdoid tumors to SMARCB1 implies a second locus for the rhabdoid tumor predisposition syndrome. *Pediatr Blood Cancer* **47**:273–278.
10. Gardner SL, Asgharzadeh S, Green A, Horn B, McCowage G, Finlay J (2008) Intensive induction chemotherapy followed by high dose chemotherapy with autologous hematopoietic progenitor cell rescue in young children newly diagnosed with central nervous system atypical teratoid rhabdoid tumors. *Pediatr Blood Cancer* **51**:235–240.
11. Gessi M, Giangaspero F, Pietsch T (2003) Atypical teratoid/rhabdoid tumors and choroid plexus tumors: when genetics "surprise" pathology. *Brain Pathol* **13**:409–414.
12. Haberler C, Laggner U, Slavc I, Czech T, Ambros IM, Ambros PF *et al* (2006) Immunohistochemical analysis of INI1 protein in malignant pediatric CNS tumors: lack of INI1 in atypical teratoid/rhabdoid tumors and in a fraction of primitive neuroectodermal tumors without rhabdoid phenotype. *Am J Surg Pathol* **30**:1462–1468.
13. Hasselblatt M, Böhm C, Tatenhorst L, Dinh V, Newrzella D, Keyvani K *et al* (2006) Identification of novel diagnostic markers for choroid plexus tumors: a microarray-based approach. *Am J Surg Pathol* **30**:66–74.
14. Hewitt KJ, Agarwal R, Morin PJ (2006) The claudin gene family: expression in normal and neoplastic tissues. *BMC Cancer* **6**:186.
15. Isakoff MS, Sansam CG, Tamayo P, Subramanian A, Evans JA, Fillmore CM *et al* (2005) Inactivation of the Snf5 tumor suppressor stimulates cell cycle progression and cooperates with p53 loss in oncogenic transformation. *Proc Natl Acad Sci USA* **2**:17745–17750.
16. Judkins AR, Mauger J, Ht A, Rorke LB, Biegel JA (2004) Immunohistochemical analysis of hSNF5/INI1 in pediatric CNS neoplasms. *Am J Surg Pathol* **28**:644–650.
17. Judkins AR, Burger PC, Hamilton RL, Kleinschmidt-DeMasters B, Perry A, Pomeroy SL *et al* (2005) INI1 protein expression distinguishes atypical teratoid/rhabdoid tumor from choroid plexus carcinoma. *J Neuropathol Exp Neurol* **64**:391–397.
18. Kalpana GV, Marmon S, Wang W, Crabtree GR, Goff SP (1994) Binding and stimulation of HIV-1 integrase by a human homolog of yeast transcription factor SNF5. *Science* **266**:2002–2006.
19. Kato H, Honma R, Sanda T, Fujiwara T, Ito E, Yanagisawa Y *et al* (2007) Knock down of hSNF5/Ini1 causes cell cycle arrest and apoptosis in a p53-dependent manner. *Biochem Biophys Res Commun* **361**:580–585.
20. Louis DN, Ohgaki H, Weistler OD, Cavenee WK (2007) *WHO Classification of Tumours of the Central Nervous System*, 4th edn. IARC Press: Lyon.
21. Medjkane S, Novikov E, Versteege I, Delattre O (2004) The tumor suppressor hSNF5/INI1 modulates cell growth and actin cytoskeleton organization. *Cancer Res* **64**:3406–3413.
22. Modena P, Lualdi E, Facchinetti F, Galli L, Teixeira MR, Pilotti S, Sozzi G (2005) SMARCB1/INI1 tumor suppressor gene is frequently inactivated in epithelioid sarcomas. *Cancer Res* **65**:4012–4019.
23. Morozov A, Lee SJ, Zhang ZK, Cimica V, Zagzag D, Kalpana GV (2007) INI1 induces interferon signaling and spindle checkpoint in rhabdoid tumors. *Clin Cancer Res* **13**:4721–4730.
24. Oliveira SS, Morgado-Díaz JA (2007) Claudins: multifunctional players in epithelial tight junctions and their role in cancer. *Cell Mol Life Sci* **64**:17–28.
25. Patil S, Perry A, Maccollin M, Dong S, Betensky RA, Yeh TH *et al* (2008) Immunohistochemical analysis supports a role for INI1/SMARCB1 in hereditary forms of schwannomas, but not in solitary, sporadic schwannomas. *Brain Pathol* **18**:517–519.
26. Pomeroy SL, Tamayo P, Gaasenbeek M, Sturla LM, Angelo M, McLaughlin ME *et al* (2002) Prediction of central nervous system embryonal tumour outcome based on gene expression. *Nature* **415**:436–442.
27. Quan C, Lu SJ (2003) Identification of genes preferentially expressed in mammary epithelial cells of Copenhagen rat using subtractive hybridization and microarrays. *Carcinogenesis* **24**:1593–1599.
28. Reddy AT (2005) Atypical teratoid/rhabdoid tumors of the central nervous system. *J Neurooncol* **75**:309–313.
29. Rorke LB, Packer R, Biegel J (1995) Central nervous system atypical teratoid/rhabdoid tumors of infancy and childhood. *J Neurooncol* **24**:21–28.
30. Rorke LB, Packer RJ, Biegel JA (1996) Central nervous system atypical teratoid/rhabdoid tumors of infancy and childhood: definition of an entity. *J Neurosurg* **85**:56–65
31. Smyth GK (2004) Linear models and empirical bayes methods for assessing differential expression in microarray experiments. *Stat Appl Genet Mol Biol* **3**:Article 3.
32. Swisshelm K, Macek R, Kubbies M (2005) Role of claudins in tumorigenesis. *Adv Drug Deliv Rev* **57**:919–928.
33. Troy TC, Arabzadeh A, Yerlikaya S, Turksen K (2007) Claudin immunolocalization in neonatal mouse epithelial tissues. *Cell Tissue Res* **330**:381–388.
34. Turksen K, Troy TC (2001) Claudin-6: a novel tight junction molecule is developmentally regulated in mouse embryonic epithelium. *Dev Dyn* **222**:292–300.
35. Versteege I, Sévenet N, Lange J, Rousseau-Merck MF, Ambros P, Handgretinger R *et al* (1998) Truncating mutations of hSNF5/INI1 in aggressive paediatric cancer. *Nature* **394**:203–206.
36. Wu Z, Irizarry R, Gentleman R, Martinez Murillo F, Spencer F (2004) A model-based background adjustment for oligonucleotide expression arrays. *J Am Stat Assoc* **99**:909–917.
37. Wyatt-Ashmead J, Kleinschmidt-DeMasters B, Mierau GW, Malkin D, Orsini E, McGavran L, Foreman NK (2001) Choroid plexus carcinomas and rhabdoid tumors: phenotypic and genotypic overlap. *Pediatr Dev Pathol* **4**:545–549.
38. Zhang ZK, Davies KP, Allen J, Zhu L, Pestell RG, Zagzag D, Kalpana GV (2002) Cell cycle arrest and repression of cyclin D1 transcription by INI1/hSNF5. *Mol Cell Biol* **22**:5975–5988.
39. Zhao L, Yaoita E, Nameta M, Zhang Y, Cuellar LM, Fujinaka H *et al* (2008) Claudin-6 localized in tight junctions of rat podocytes. *Am J Physiol Regul Integr Comp Physiol* **294**:R1856–R1862.
40. Zimmerman MA, Goumnerova LC, Proctor M, Scott RM, Marcus K, Pomeroy SL *et al* (2005) Continuous remission of newly diagnosed and relapsed central nervous system atypical teratoid/rhabdoid tumor. *J Neurooncol* **72**:77–84.